[8]D. C. Burnham and R. Y. Chiao, Phys. Rev. 188, 667 (1969); S. L. McCall, thesis, University of California, 1968 (unpublished).

[9]J. C. MacGillivray and M. S. Feld, Phys. Rev. A 14, 1169 (1976).

[10]A numerical integration of Eq. (5.16) of Ref. 5 gives $\mu = 0.78\ [(3/8\pi)/(\lambda^2/A)]$ for $\lambda = 2931$ nm, $L = 2$ cm, and $F = 1$, but this 0.78 correction has not been applied to any value of τ_R quoted herein.

[11]M. Gross, C. Fabre, P. Pillet, and S. Haroche, Phys. Rev. Lett. 36, 1035 (1976); A. Flusberg, T. Mossberg, and S. R. Hartmann, Phys. Lett. 58A, 373 (1976).

[12]Without a magnetic field several sublevels of $7P_{3/2}$ are excited leading to beats in the SF output: Q. H. F. Vrehen, H. M. J. Hikspoors, and H. M. Gibbs, Phys. Rev. Lett. 38, 764 (1977).

[13]The dipole moments (Ref. 2) for the strongest transitions are, in 10^{-18} esu cm, $d_{SF} = 12$, $d_{pump} = 0.5$, $d_{7P-5D} = 1.75$, and $d_{7S-6P} = 4.4$.

[14]S. Svanberg and S. Rydberg, Z. Phys. 227, 216 (1969); P. W. Pace and J. B. Atkinson, Can. J. Phys. 53, 937 (1975); O. S. Heavens, J. Opt. Soc. Am. 51, 1058 (1961). The $7P_{3/2}$ to $7S_{1/2}$ partial lifetime is 275.5 ns; since the $\Delta m_J = +1$ SF transition emits perpendicular to the magnetic field, the effective lifetime must be doubled. The relaxation times are calculated as follows. The upper state a of the SF transition may decay to the lower state b or to other states c; b may decay to lower states d. Using the experimental value $\tau_a = 135$ ns, Heaven's calculated value $\tau_b = 57$ ns, and Heaven's branching ratios, one has $\tau_{ab} = 275.5$ ns, $\tau_{ac} = 264.7$ ns, and $\tau_{bd} = 57$ ns. A straightforward extension of the three-level decay formulas in R. E. Slusher and H. M. Gibbs, Phys. Rev. A 5, 1634 (1972), yields $1/T_1 = 1/\tau_{ab} + 1/2\tau_{ac} + 1/2\tau_{bd}$ and $1/T_2' = 1/2\tau_a + 1/2\tau_b$ for the energy and coherence relaxation rates.

[15]Q. H. F. Vrehen, in *Cooperative Effects in Matter and Radiation*, edited by C. M. Bowden, D. W. Howgate, and H. R. Robl (Plenum, New York, 1977).

[16]Although the pump pulse is neither coherent nor completely incoherent, it is believed that saturation occurs rather than coherent excitation. This conclusion is mainly based on the following observations: (a) τ_D decreases monotonically with increasing pump power and converges to an asymptotic value at the highest pump power; (b) in an additional experiment the pulse duration was increased to 3 ns and the bandwidth to 1200 MHz without either quantitative or qualitative changes in the SF output pulses for a 1-cm cell.

[17]R. Saunders, S. S. Hassan, and R. K. Bullough, J. Phys. A 9, 1725 (1976).

[18]H. M. Gibbs, B. Bölger, F. P. Mattar, M. C. Newstein, G. Forster, and P. E. Toschek, Phys. Rev. Lett. 37, 1743 (1976).

Stochastic Ion Heating by a Perpendicularly Propagating Electrostatic Wave

C. F. F. Karney and A. Bers

Research Laboratory of Electronics and Plasma Fusion Center, Massachusetts Institute of Technology, Cambridge, Massachusetts 02139

(Received 29 November 1976)

The motion of an ion in the presence of a constant magnetic field and a perpendicularly propagating electrostatic wave with frequency several times the ion cyclotron frequency is shown to become stochastic for fields satisfying $E/B_0 > \frac{1}{4}(\Omega/\omega)^{1/3}(\omega/k)$. This stochasticity condition is independent of how close ω is to a cyclotron harmonic. Applications of current interest in supplementary heating of plasmas with rf power near the lower-hybrid frequency are suggested.

It is well known that a small- (infinitesimal-) amplitude electrostatic wave traveling across a constant magnetic field suffers linear damping on the ions only if its frequency ω is an exact multiple of the ion cyclotron frequency, Ω. At finite amplitudes of the wave, nonlinear effects become important and we can expect that this resonance is broadened. We show that a single wave leads to stochastic ion motion at an amplitude which is independent of how close ω is to a cyclotron harmonic, $n\Omega$. This provides a mechanism whereby the ions in a plasma can be heated by such coherent waves.

There are two, physically distinct, nonlinear mechanisms operative in this interaction. The first consists of a transient trapping of the ions in the potential of the wave; this leads to a rapid heating of the ions near the lower boundary of the stochastic region.[1] The second is due to nonlinear resonances that arise from the perturbed cyclotron motion of the ions in the wave field, and which produce stochastic ion motion in a region of ion velocity space extending from the trapping region to an upper bound determined by the field amplitude; this leads to a slower heating of the ions up to the upper boundary of the stochastic region.

In current schemes for the supplementary heat-

ing of tokamak plasmas with microwave power, wave-packet fields that propagate nearly across the magnetic field (e.g., lower-hybrid-resonance cones and some of their parametrically excited decay waves) are generated. The stochastic ion heating mechanism we present can play an important role in such heating schemes.

Stochastic ion motion can also be caused by an obliquely propagating wave that traps ions in the potential wells parallel to the magnetic field.[2] This mechanism is inapplicable for the wave of interest here, which we take to propagate exactly across the magnetic field.

We consider an ion in a constant magnetic field $B_0\hat{z}$ and a perpendicularly propagating electrostatic wave $\hat{y}E\cos(ky-\omega t-\varphi)$. The equations of motion are

$$\ddot{y}+\dot{x}=\alpha\cos(y-\nu t-\varphi),\quad \ddot{x}-\dot{y}=0, \tag{1}$$

where lengths are normalized to k^{-1} and times to Ω^{-1}, $\alpha=qkE/(m\Omega^2)$, and $\nu=\omega/\Omega$. The Hamiltonian for this system is

$$H=I_1+\nu I_2-\alpha\sin[(2I_1)^{1/2}\sin w_1-w_2], \tag{2}$$

where (I_1,w_1) and (I_2,w_2) are conjugate action-angle variables of the unperturbed system ($\alpha\to 0$), $y=(2I_1)^{1/2}\sin w_1$, and $x=-I_2-(2I_1)^{1/2}\cos w_1$ (without loss of generality, we take the constant of the motion, $\dot{x}-y$, to be zero). In (2) w_2 is the wave phase and so H describes two harmonic oscillators, the ion in a magnetic field described by (I_1, w_1) and the wave described by (I_2,w_2), coupled by the last term in (2).

In order to find the condition for the onset of stochasticity we use the surface-of-section method.[3] We choose the cross section defined by $w_1=\pi$ and numerically compute $r\equiv(2I_1)^{1/2}$, the normalized velocity, against w_2 for each crossing of the $w_1=\pi$ plane. Figure 1 shows the results of such computations for $\nu=30.23$, $\alpha=2.2$ and 4, and in a region of velocity space with $r>\nu$. With $\alpha=0$ the trajectories would all lie on horizontal straight lines, since I_1 is a conserved quantity. At $\alpha=2.2$ the trajectories have become quite complex, many lying on chains of "islands." The order of the islands is given by the number of cyclotron orbits it takes for the ion to return to the island it started on. Clearly visible are chains of fourth- and fifth-order islands. Outside the islands the motion appears stochastic, but the stochastic regions are separated from one another by coherent regions, preventing the movement of particles from one stochastic region to another and limiting the amount of energy the particles

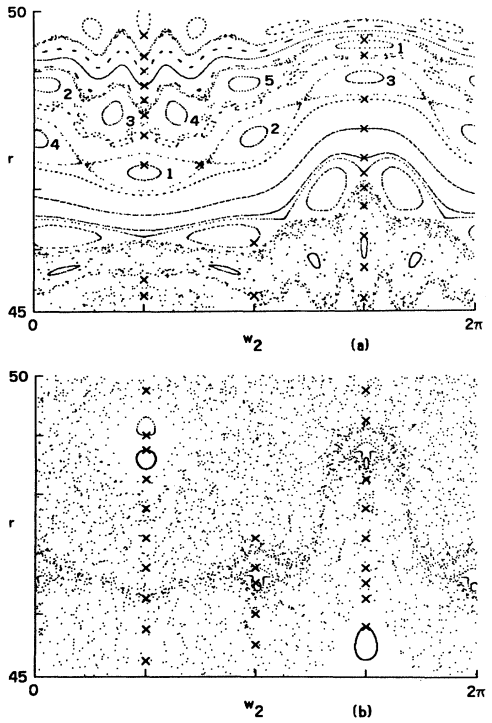

FIG. 1. The $w_1=\pi$ cross sections of phase space for $\nu=30.23$ and (a) $\alpha=2.2$, (b) $\alpha=4$. The trajectories of 24 particles are followed for 300 orbits in each case. Crosses indicate initial conditions; dots, subsequent crossings. In (a) the numbers indicate the position of fourth- and fifth-order islands and the order in which they are visited. The initial conditions were picked to illustrate the dominant features of the motion.

can gain. At $\alpha=4$, the motion is stochastic over nearly all of the region of velocity space shown in the figure, allowing particles to be heated through the region.

From the study of these figures and others at different frequencies, we form the following picture of how the motion becomes stochastic: The presence of the wave causes a nonlinear change in the cyclotron frequency, $\langle\dot{w}_1\rangle$. This in turn causes the ratio of the wave frequency to the cyclotron frequency to become a "simple" rational number in certain regions of velocity space, leading to fixed points. [In Fig. 1(a), for instance, the cyclotron frequency has become $\nu/30\frac{1}{4}$ and $\nu/30\frac{1}{5}$ at the fourth- and fifth-order islands, respectively.] Around half of these fixed points, a chain of islands forms; the other half are hyperbolic fixed points at the separatrices between the islands. As is well known,[3,4] the addition of any small perturbation to the system causes the motion in the vicinity of the separatrix to become sto-

chastic [see Fig. 1(a)]. At what we define to be the "stochasticity threshold" the chains of islands of various orders overlap, causing the stochasticity to become much more widespread [see Fig. 1(b)]; above this threshold appreciable heating is possible. As the field is increased two factors contribute to the eventual overlap of the islands. Firstly, the islands grow in size (although this effect is not always visible in surface-of-section plots because the size of the stochastic regions surrounding the islands also increases, eating away at the islands). Secondly, and perhaps more significantly for our problem, islands of different orders appear.

To find the stochasticity threshold in terms of island overlap, we should therefore do two things: to find out at what field the islands of various orders appear, and to find out their size. As we will see, all but first-order islands appear as the result of an $O(\alpha^2)$ shift in the frequency. The size of the corresponding islands is determined by higher-order terms. The following analysis gives the threshold for islands of various orders, but not their size. This together with the numerical simulations gives us the stochasticity threshold.

The location of pth-order islands may be derived analytically by finding pth-order fixed points. These in turn are found by setting

$$\langle \dot{w}_1 \rangle / \dot{w}_2 = \langle \dot{w}_1 \rangle / \nu = p/s, \tag{3}$$

where s and p are integers and the (time) average is performed over p cyclotron orbits (or, equivalently, s wave periods). For first-order islands ($p=1$, $s=n$), $\langle \dot{w}_1 \rangle$ is readily found by a Fourier transformation[5] of (2) with respect to w_1 and w_2. Then to order α, $nw_1 - w_2$ is constant, and so only one term in the Fourier sum contributes to give

$$\langle \dot{w}_1 \rangle = 1 - \alpha(\partial/\partial I_1) J_n[(2I_1)^{1/2}] \sin(nw_1 - w_2). \tag{4}$$

To find the threshold for first-order islands we substitute (4) in (3) and take $\sin(nw_1 - w_2) = \pm 1$. If we also asymptotically expand the Bessel function in the limit $r \gg \nu$, we obtain

$$\alpha = (\tfrac{1}{2}\pi r^3)^{1/2} |\delta| / n, \tag{5}$$

where $\nu = n + \delta$. For $p \neq 1$, we transform[5] H to a set of action-angle variables for which the angles are cyclic to order α. Then, if we are not too close to the threshold for first-order islands, there are contributions to H of order α^2 varying as $\sin(mw_1 - kw_2)$, where $k=0$ or 2. If $p \neq 2$, then on averaging only the angle-independent term ($m = k = 0$) contributes, giving

$$\langle \dot{w}_1 \rangle = 1 - \frac{\alpha^2}{4} \sum_{m=-\infty}^{\infty} \frac{\partial^2 J_m{}^2[(2I_1)^{1/2}]}{\partial I_1{}^2} \frac{m}{m-\nu}. \tag{6}$$

For $p=2$, there is an additional contribution when $m=s$ and $k=2$; however, with $r > \nu \gg 1$ and $\nu \approx n + \frac{1}{2}$, this term is negligible, so that we use (6) in this case also. In Fig. 2(a) we plot $\nu/\langle \dot{w}_1 \rangle$ as given by (6). As α is increased, the island condition, (3), is satisfied for more and more values of s and p. The threshold for a particular chain of higher-order islands is found by substituting (6) in (3). Expanding in the limit $r \gg \nu \gg 1$ gives

$$\alpha = |\sin(\pi\delta)\epsilon r^3|^{1/2}/n, \tag{7}$$

where $\nu = s/p + \epsilon$.

In Fig. 2(b) we plot the predicted values of the thresholds for island formation as given by (5) and (7) for $29\frac{1}{2} < \nu < 30\frac{1}{2}$, and $r \approx 47.5$ (in this plot we have allowed for the fact that $r \gg \nu$ is not satisfied), together with the numerically observed thresholds for various ν. Also given in Fig. 2(b) are some numerically observed stochasticity thresholds. We observe that this threshold is insensitive to δ, varying by about 20% for δ be-

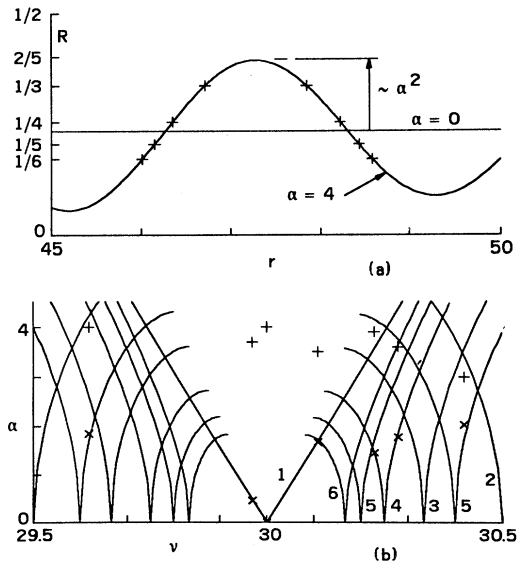

FIG. 2. (a) Plot of $R \equiv \nu/\langle \dot{w} \rangle - 30$ as given by (6) for $\nu = 30.23$. The plusses indicate the values of r for which $\langle \dot{w}_1 \rangle$ is a simple rational multiple of ν. (b) The threshold α for the formation of islands of various orders (the numbers by the curves) for $r \approx 47.5$ as a function of ν. The lines give the analytically predicted values and the crosses give the numerically observed values. The plusses give the numerically observed stochasticity thresholds.

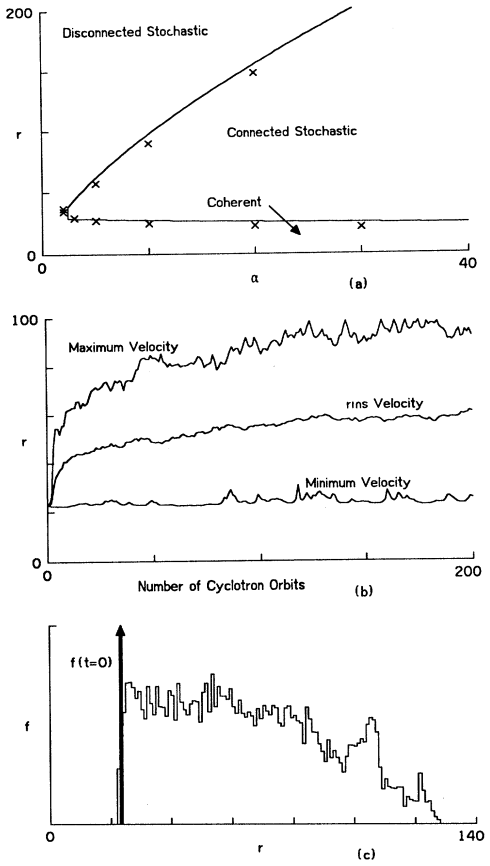

FIG. 3. (a) The limits of the stochastic region as given by Eqs. (9), (11), and (12). The crosses give the numerically observed values. The terms "disconnected stochastic" and "connected stochastic" are used to distinguish motion of the type shown in Figs. 1(a) and 1(b), respectively. (b) Heating of a group of 50 particles with $\alpha \approx 20$, initial velocity $r = 23$, and evenly distributed phases. (c) Velocity (r) distribution function for the particles in (b) averaged over orbits 800–1100. Normalization is such that $\int 2\pi r f\, dr = 1$.

tween $-\frac{1}{2}$ and $\frac{1}{2}$. Since the overlap of islands causes the motion to become stochastic, an accurate expression for the stochasticity threshold is obtained merely by replacing δ and ϵ in (5) or (7) by a constant [which we determine from Fig. 2(b)], while retaining the slow dependence on r and n, giving, for $r \gg \nu \gg 1$,

$$\alpha = (\tfrac{1}{2}\pi r^3)^{1/2}/4n. \tag{8}$$

For $r \approx \nu$, we must go back to (4) and (6) and expand in the limit $\nu \gg 1$ to obtain[6]

$$\alpha = \nu^{2/3}/4, \tag{9}$$

or, in unnormalized terms,

$$E/B_0 = \tfrac{1}{4}(\Omega/\omega)^{1/3}(\omega/k). \tag{10}$$

Our results can be used to determine what region of velocity space is stochastic for a given α. For α much larger than the threshold given by (9), the upper limit may be found by inverting (8) to give

$$r = (4\alpha n)^{2/3}(2/\pi)^{1/3}. \tag{11}$$

The lower limit is determined by trapping[1] and so is given by

$$r = \nu - \sqrt{\alpha}. \tag{12}$$

Figure 3(a) shows these limits for $\nu = 30.23$, together with the numerically observed values. How an ion gains energy within the stochastic region may be illustrated by integrating the equations for a number of ions with velocities just above the lower limit of the stochastic region and with evenly distributed phases. In Fig. 3(b) we plot the rms speed of 50 particles as a function of cyclotron-orbit number (which is nearly proportional to time) for $\alpha = 20$ and $\nu = 30.23$. We note that the fairly rapid initial energy gain is followed by a slower heating. We can attribute the initial energy gain to the effects of trapping. Indeed, the rms velocity after the first few cyclotron orbits is close to $\nu + 2\sqrt{\alpha}$. The slow heating continues for longer than 1000 cyclotron orbits, at which time the rms velocity is about 90, and the velocity distribution function has spread over most of the stochastic region, Fig. 3(c).

As an example, consider a wave near the lower-hybrid frequency in a plasma with $n_0 = 10^{14}$ cm^{-3}, $B_0 = 50$ kG, and $T_i = 1$ keV. Taking $\omega/\Omega_i \equiv \nu = 24$, and $k_\perp v_{Ti}/\Omega_i = 6$, we find from (10) that the threshold field for stochasticity is about 5.5 keV/cm (at this field $\epsilon_0 E^2/4n_0 T_i$ is about 4×10^{-5}). The motion becomes stochastic for particles traveling at the wave phase velocity which is $4v_{Ti}$ so that an appreciable number of tail particles is heated. In tokamaks the lower-hybrid wave is of finite extent, determined by the excitation structure. In this example, if the extent along B_0 is 10 cm, then the ions spend about 20 cyclotron periods in this field and can increase their energy by an amount corresponding to the trapping width of the fields. At much higher amplitudes of the lower-hybrid fields, the conditions for parametric decay may also be satisfied. For the decay waves which are of lower frequency and shorter wavelength, the conditions for stochastic ion heating (10) and (12) may be more readily sat-

isfied even for ions with velocities nearer to v_{Ti} so that bulk ion heating can result.

This work was supported by the U. S. Energy Research and Development Administration under Contract No. E(11-1)-3070.

[1]C. F. F. Karney, A. Bers, and D. C. Watson, Bull. Am. Phys. Soc. 20, 1313 (1975); C. F. F. Karney and A. Bers, M.I.T. Plasma Research Reports No. 76/7, 1976, and No. 76/24, 1976 (unpublished).

[2]G. R. Smith and A. N. Kaufman, Phys. Rev. Lett. 34, 1613 (1975).

[3]G. M. Zaslavskii and B. V. Chirikov, Usp. Fiz. Nauk 105, 3 (1971) [Sov. Phys. Usp. 14, 549 (1972)].

[4]J. Ford, in *Fundamental Problems in Statistical Mechanics*, edited by E. D. G. Cohen (North-Holland, Amsterdam, 1975), Vol. 3.

[5]G. H. Walker and J. Ford, Phys. Rev. 188, 416 (1969).

[6]This result may also be obtained (to within a factor of order unity) by demanding that trapping be effective, in the sense that an ion in its orbit spends at least a bounce period ($2\pi\alpha^{-1/2}$) within the trapping region given by $|\dot{y}-\nu|<\sqrt{\alpha}$.

Anomalous Thermal Properties of Glasses

W. H. Tanttila
Department of Physics and Astrophysics, University of Colorado, Boulder, Colorado 80309
(Received 28 January 1977)

Experiments have shown that glasses, at low temperatures, possess an anomalous specific heat above that due to the lattice vibrations. Using two parameters I fit the contribution of a new excitation to the experimental specific-heat data. An experiment to test the theory is suggested.

The low-temperature specific heat of glass has been reported[1] to have an anomaly in that it is "excessive." This excess is above the T^3 dependence from lattice waves that one normally finds in crystals. Several explanations have been offered for this "excess" specific heat. In one assignment the "excess" specific heat has been attributed to localized low-frequency oscillations of molecules at voids[2] or to a localized two-level system.[3] Another explanation is that the excessive specific heat arises from the excitation of defects of the dislocation type.[4] In another explanation Fulde and Wagner[5] have constructed a propagator for low-lying phonons that is the basis of a semiphenomenological model into which they insert decay properties of these phonons. Takeno and Goda[6] show a contribution from the extra density of states from rotonlike excitations. To my knowledge there has been no experiment that unequivocally eliminates these explanations. I offer here an explanation similar to that of Takeno and Goda, which gives rather good agreement with some of the experimental results and is consistent with a general hypothesis concerning liquids and glasses that I have formulated[7] and with which I have had some good success in assessing numerous properties of liquids.

Stephens[1] has suggested that perhaps the phonon picture is not useful to describe the specific heat and heat conductivity of glasses and has suggested that another representation is needed. Zeller and Pohl[1] likewise have suggested that the anomaly in glass is specific to the amorphous state. My treatment is consistent with both of these points of view. In my treatment I propose that all liquids and glasses possess a new fundamental excitation.

This excitation is a localized region of somewhat lower density than the host matrix. Corre-

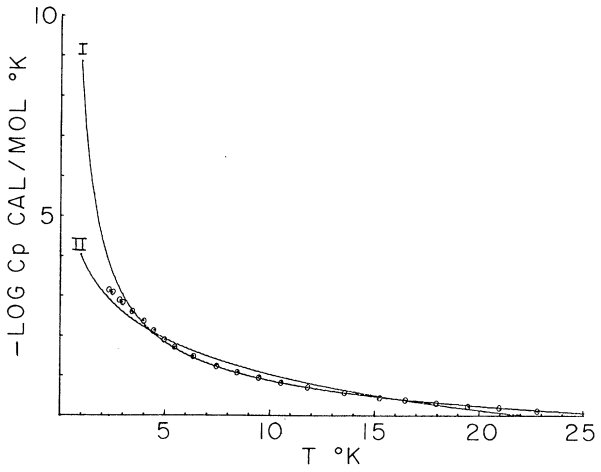

FIG. 1. Experimental values (Ref. 7) (circles) for $\ln C_p$ as a function of temperature. Curve I is from Eq. (2), and curve II is from kT^3 fitted at $T = 15.147$°K. Note the departure of the experimental points from the theoretical curve I beginning between 3 and 4°K.